

## Biodegradable dissolved organic matter in a temperate and a tropical stream determined from ultra-high resolution mass spectrometry

*Sunghwan Kim*<sup>1</sup>

Department of Chemistry, The Ohio State University, Columbus, Ohio 43210

*Louis A. Kaplan*

Stroud Water Research Center, Avondale, Pennsylvania 19311, and Department of Biology, University of Pennsylvania, Philadelphia, Pennsylvania 19104

*Patrick G. Hatcher*<sup>2</sup>

Department of Chemistry, The Ohio State University, Columbus, Ohio 43210

### *Abstract*

We investigated dissolved organic matter (DOM) metabolism by employing plug-flow biofilm reactors and ultra-high resolution mass spectrometry of DOM isolated by C<sub>18</sub> extraction in two forested stream ecosystems, a low DOM tropical stream sampled at baseflow and a higher DOM temperate stream sampled during a storm. On passage through the bioreactors, DOM concentrations in the tropical stream sample declined by 22%, whereas they declined by 42% in the temperate stream sample. The extracted DOM was subjected to electrospray ionization coupled to Fourier transform ion cyclotron resonance mass spectrometry to obtain information on molecular weight distributions and elemental compositions for the thousands of compounds whose masses are calculated with sufficient accuracy to allow calculation of unique elemental formulas. In both streams, metabolism modifies DOM to lower molecular weight molecules, and oxygen-rich molecules are selectively biodegraded. Applying van Krevelen analyses for the unique elemental formulas of DOM constituents revealed that hydrogen-deficient molecules with low H:C ratios (assigned to black carbon-derived molecules) are present and generally not metabolized. Black carbon molecules are refractory to biodegradation compared with other components of DOM, supporting the suggestion that black carbon molecules in DOM flow to the ocean without experiencing significant microbial degradation.

Dissolved organic matter (DOM) provides energy and carbon for microorganisms in aquatic ecosystems, especially heterotrophic bacteria. Understanding controls on the processes of DOM uptake and metabolism enhances our understanding of aquatic food webs. Similarly, describing the chemical composition of the biodegradable component of DOM (BDOM) helps clarify how heterotrophic bacteria obtain energy and nutrients. Consequently, there have been numerous studies on the utilization of DOM by microorganisms where bioassays, combined with bulk parameters and molecular-level parameters, have been used to study the biologically labile portion of DOM.

Bulk parameters such as DOC concentration, elemental composition, oxidation state of DOM, and dissolved oxygen concentration, as well as molecular-level analyses such as

neutral sugar and amino acid concentrations and compositions, Fourier transform infrared spectroscopy (FT-IR), NMR spectroscopy, and <sup>12</sup>C:<sup>13</sup>C tetramethylammonium hydroxide (TMAH) thermochemolysis coupled to gas chromatography (GC) have successfully described the link between bacteria and DOM. These studies have characterized the biologically labile portion of DOM; they indicated that microorganisms utilize a broad range of compounds, including amino acids, carbohydrates, humic substances, fatty acids, and lignin, and showed that microbial degradation processes significantly alter the chemical composition of DOM (Volk et al. 1997; Frazier et al. 2005). Yet these studies do not provide a full molecular-level description of DOM or BDOM composition, especially the hydrophobic constituents, so that the chemistry and molecular composition of this important C and energy source within aquatic ecosystems remains poorly understood.

DOM exhibits an exceptionally high degree of complexity, and this poses analytical challenges for a broad-spectrum characterization of the molecular composition of DOM that few analytical tools are capable of providing. In streams, the complexity of DOM is due to the diversity of allochthonous (terrestrial vegetation and soil leachates) and autochthonous (algae, macrophytes, heterotrophs) sources and compounded by digenetic alterations from geo-, photo-, and biochemical reactions. The combination of molecular complexity and analytical limitations make it difficult to answer fundamental questions concerning the molecular composi-

<sup>1</sup> Present address: Korean Basic Science Institute, 52 Eoeun-dong, Yuseong-gu, Daejeon 305-333.

<sup>2</sup> Corresponding author. Present address: Department of Chemistry, Old Dominion University, Norfolk, Virginia 23529 (phatcher@odu.edu).

### *Acknowledgments*

Sherman Roberts, Michael Gentile, Raphael Morales, and Christian Collado assisted in sample collection and processing. We thank Alan G. Marshall, Ryan P. Rodgers, and Zhigang Wu at the National High Magnetic Field Laboratory (CHE-9903528) for their assistance in FT-ICR analysis. This research was supported by NSF DEB 9904047, NSF DEB 0096276, and the Stroud Endowment for Environmental Research.

tion of DOM and BDOM. This underscores a need in organic matter biogeochemistry to apply a new powerful analytical technique such as electrospray ionization (ESI) Fourier transform ion cyclotron resonance mass spectrometry (FT-ICR-MS), which has been found to provide high-resolution capability for complex mixtures (Kujawinski et al. 2002; Stenson et al. 2003).

Although there have been attempts to obtain molecular-level details on the composition of DOM by use of ESI coupled to low-resolution mass spectrometric techniques (Seitzinger et al. 2005), the molecular complexity of DOM leads to the existence, in ESI-MS, of numerous mass spectral peaks at each nominal mass that can only be resolved by use of FT-ICR-MS (Kujawinski et al. 2002). FT-ICR-MS has been used to analyze Suwannee River fulvic acid (Kujawinski et al. 2002; Stenson et al. 2003), DOM from the Rio Negro tributary of the Amazon River and McDonalds Branch within the New Jersey Pinelands (Kim et al. 2004), and oceanic DOM (Koch et al. 2005). FT-ICR-MS of DOM produces complicated mass spectra that can be used to estimate molecular weight, identify patterns of elemental composition, and calculate weighted H:C and O:C ratios (Kim et al. 2003a). Here we present data for stream waters from widely different ecosystems that were subjected to bioassays. FT-ICR-MS analyses of DOM from bioreactors allowed us to examine the changes in DOM molecular composition induced by microbial decomposition.

## Methods

*Study sites*—We conducted these studies with stream water and microorganisms from two different forested biomes, Rio Tempisque within the evergreen tropics of Guanacaste Province, northwestern Costa Rica, and White Clay Creek, within a temperate deciduous watershed in southeastern Pennsylvania. Headwaters of Rio Tempisque drain a dense, virgin forest and are characterized by low median baseflow concentrations ( $0.7 \text{ mg C L}^{-1}$ ) of dissolved organic carbon (DOC), neutral pH (7.8–8.6), low conductivity ( $74\text{--}82 \mu\text{S cm}^{-1}$ ), low to moderate nutrient concentrations ( $0.14\text{--}0.26 \text{ mg NO}_3^{-1}\text{-N L}^{-1}$ ;  $8\text{--}14 \mu\text{g PO}_4^{-3}\text{-P L}^{-1}$ ) and narrow temperature ranges ( $21\text{--}22^\circ\text{C}$ ). White Clay Creek drains a third-order agricultural watershed with an intact riparian forest and is characterized by a moderate median baseflow DOC concentration ( $1.5 \text{ mg C L}^{-1}$ ), neutral pH (7.5–8.3), moderate conductivity ( $176\text{--}218 \mu\text{S cm}^{-1}$ ), nutrient enrichment ( $4.3\text{--}5.2 \text{ mg NO}_3^{-1}\text{-N L}^{-1}$ ;  $4\text{--}33 \mu\text{g PO}_4^{-3}\text{-P L}^{-1}$ ), and a broad temperature range ( $0\text{--}24^\circ\text{C}$ ).

*Biofilm reactors*—Some of the waters from Rio Tempisque and White Clay Creek are diverted into “wet” laboratories adjacent to each stream for experiments, and those stream water supplies were used to colonize and maintain bioreactors at each site. The bioreactors were constructed from paired glass chromatography columns (Chromaflex, Kontes, 25 mm diameter  $\times$  600 mm; total volume 589 mL) filled with 1–2 mm diameter sintered borosilicate glass beads with 60–300  $\mu\text{m}$  pore diameters (Siran Schott) connected in series and were continuously fed with filtered stream water in a once-through, upflow mode at  $4 \text{ mL min}^{-1}$  (Kaplan and

Newbold 1995). The water-jacketed bioreactors were kept at ambient stream temperatures by a constant flow of stream water and were shielded with aluminum foil to eliminate light. Prior studies have demonstrated that once colonized, the bioreactors equilibrate rapidly to changes in feed water DOC concentrations through adsorption and desorption reactions (Kaplan and Newbold 1995). Stream water, which provided a continual inoculum of colonizing bacteria, energy, and nutrients, was filtered through a series of high-temperature cured, glass fiber cartridges (0.3, 25, and 75  $\mu\text{m}$ ; Balston) and stored in covered polyethylene reservoirs. Direct microscopic counts of Balston-filtered and unfiltered water showed that 95% of suspended bacteria passed through the filters into the feed water (Kaplan unpubl. data). Reservoirs were replenished once a week, and the bioreactors were colonized for a minimum of 6 months prior to sampling. Biodegradable DOC (BDOC) concentrations were calculated as the difference between DOC in the influent and effluent water, although we know that these measurements of net changes in DOC concentration underestimate BDOC concentrations due to DOC excreted by bacteria within the bioreactors (Kaplan and Newbold 1995). For the measurements reported here, the bioreactors were switched from reservoir water to freshly collected and filtered stream water. The White Clay Creek samples were collected during the falling limb of a November storm that increased discharge 4.5-fold over baseflow (water temperature =  $11^\circ\text{C}$ ), and the Rio Tempisque samples were collected at baseflow during March in the middle of the dry season (water temperature =  $20^\circ\text{C}$ ). Bioreactor outflow samples were collected after two bed volumes (1.2 L) had eluted to assure that the columns were filled with the test water. Four replicate bioreactors were used for each of the streams, with the effluent waters pooled in a covered vessel held in an ice bath.

*Chemical analyses*—DOC measurements were performed on bioreactor influent and effluent waters by ultraviolet-promoted persulfate oxidation and membrane conductometric detection (Sievers 800 TOC analyzer equipped with an inorganic carbon removal module, Ionics Instrument). Mass spectrometric analyses were performed on bioreactor samples following acidification and  $\text{C}_{18}$  solid phase extraction (Kim et al. 2003b). Water samples were adjusted to pH 2–3 with hydrochloric acid (ACS grade, Fisher Scientific) and passed through a  $\text{C}_{18}$  solid phase extraction disk that had been pre-activated in methanol and washed with ultrapure water. The organic material retained on the  $\text{C}_{18}$  solid phase extraction disk was rinsed and eluted twice with 10 mL of 90:10 MeOH:H<sub>2</sub>O solution and stored in a refrigerator to reduce evaporation of the solvent. Previous studies (Kim et al. 2003b) with DOM from a blackwater stream in the Pine Barrens, New Jersey, show that the  $\text{C}_{18}$  approach recovers approximately 60% of the DOM. Calculation of recoveries requires the use of a UV-visible spectrophotometer, which was not available on site. Therefore, we did not estimate DOM recovery for the samples. Because the same exact extraction procedure was employed for samples collected during the present study, we assumed that recoveries would be similar for each sample. The extracted samples, now in 90:10 MeOH:H<sub>2</sub>O, were analyzed with a 9.4 Tesla FT-ICR

mass spectrometer at the National High Magnetic Field Laboratory (Tallahassee, Florida) as described previously (Kim et al. 2003a). Samples were introduced by a syringe pump through the microelectrospray ionization source at a rate of 350 nL min<sup>-1</sup>. All of the samples were analyzed in negative ionization mode with a needle voltage of -1.8 kV. Ions were stored in an octapole ion trap for 45 s before being transferred to a Penning trap. Approximately 200 time domain signals were added for a time period of approximately 5 h. The summed FID signal was zero-filled once and Hanning apodized before being processed by magnitude computation mode Fourier transformation. The bioreactor inflow and outflow samples from the same river system were analyzed sequentially to maintain near-identical experimental conditions.

Procedures for mass calibration, crucial to the assignment of precise elemental composition for peaks in the mass spectra, were performed in two steps. First, an internal calibration standard (polyethylene glycol solution of 600 Da average molecular weight; Sigma) was injected into the FT-ICR cell along with the sample by dual spray injection. The peaks in the resultant spectrum were calibrated by reference to the exact mass to charge ( $m/z$ ) of the internal calibration standard material. Second, the sample was analyzed without the polyethylene glycol internal standard to eliminate possible peak contributions from the internal standard material. The  $m/z$  scale of the mass spectrum was first calibrated by use of an external calibration standard (G2421A electrospray "tuning mix," Agilent) and then by the exact  $m/z$  numbers of major sample peaks obtained from the first spectrum.

The weight-average molecular weight ( $M_w$ ) and number-average molecular weight ( $M_n$ ) were calculated from the mass spectra using Eqs. 1 and 2 below (Brown and Rice 2000):

$$M_w = \frac{\sum_n (I_n M_n^2)}{\sum_n (I_n M_n)} \quad (1)$$

$$M_n = \frac{\sum_n (I_n M_n)}{\sum_n (I_n)} \quad (2)$$

where  $M$  is the observed molecular weight of a peak in a given mass spectrum, and  $I$  is the relative intensity of the peak.

The elemental compositions of peaks exceeding 5% of base peak threshold at odd mass were calculated from the corresponding exact mass numbers obtained from the calibrated mass spectra (Kim et al. 2003b). Peaks at an even nominal mass were mainly attributed to the isotope peaks of those at odd nominal mass ( $M-H$ ) and were, therefore, not utilized for assignment of elemental composition. C, H, O, and N atoms were used to assign the most probable elemental formulas. The peaks (especially the peaks with the molecular weight <480 Da) in mass spectra can be uniquely assigned to elemental compositions with usually <1 ppm error. In the case of the peaks in the higher molecular weight (>480 Da) portion of the spectrum, assignment to more than one elemental formula is possible. In such cases, Kendrick mass defect analysis was used to determine the assigned elemental formula as previously described (Kim et al. 2004). Briefly, in the assignment procedure, homologous series (e.g., CH<sub>2</sub> series) of peaks are identified in Kendrick mass

defect analysis, and if several possible elemental formulas match the exact mass assignment, the one selected as most probable is the formula that constitutes part of a Kendrick mass defect series.

Qualitative analyses of major classes of compounds that comprise the ultra-high resolution spectra were determined from plots of the elemental composition data on a van Krevelen plot (H:C vs. O:C), as major biomolecular components of source materials occupy fairly specific locations on the plots (van Krevelen 1950). The van Krevelen diagrams were presented as two-dimensional projections of three-dimensional plots by using peak intensities in high-resolution mass spectra as the third axis.

## Results and discussion

*DOC analyses*—The BDOC concentration from Rio Tempisquito was 0.12 ± 0.01 mg C L<sup>-1</sup> (mean ± SD,  $n = 3$  replicate bioreactors), representing 22% of the baseflow stream water DOM, based on a mean inflow concentration of 0.54 ± 0.01 mg C L<sup>-1</sup> (mean ± SD,  $n = 3$  replicate samples) and a mean outflow concentration of 0.42 ± 0.01 mg C L<sup>-1</sup>. White Clay Creek was sampled during a storm, and the BDOC concentration was 2.48 ± 0.03 mg C L<sup>-1</sup> (mean ± SD,  $n = 4$  replicate bioreactors), representing 42% of the stream water DOM, based on a mean inflow concentration of 5.85 ± 0.02 mg C L<sup>-1</sup> (mean ± SD,  $n = 3$  replicate samples) and a mean outflow concentration of 3.37 ± 0.02 mg C L<sup>-1</sup>. These BDOC concentrations are within the range of values for stream water reported with bioreactors (Volk et al. 1997), show a high degree of consistency among replicate bioreactors, and confirm that the bioreactor communities were acclimated to metabolize the DOC present in the respective stream waters.

Despite high rates of terrestrial primary productivity associated with seasonally dry tropical forests (Whittaker and Likens 1973), the DOC concentrations in Rio Tempisquito were at the low end of the spectrum of DOC concentrations reported for streams worldwide, especially within the tropics (Brinson 1976). In contrast, the DOC concentrations from White Clay Creek, with hay and row crop agriculture upslope from forested riparian buffers, were considerably higher, and for the particular sample analyzed, influenced by runoff associated with a storm. Whether the Rio Tempisquito concentrations are low because the terrestrial watershed tightly conserves carbon, the DOC lost from the forests is rapidly decomposed within the stream, high levels of precipitation dilute terrestrial DOC concentrations, or some combination of these factors, is unknown. However, adsorption and subsequent decomposition of the BDOC fraction percolating through soils is likely high within the Tempisquito watershed due to the combined effects of soil clay content, uniformly high temperatures, and N and P availability in Guancaste soils (Morera 1983).

We know from prior molecular characterization of BDOC in our study streams using bioreactors and tetramethylammonium hydroxide thermochemolysis (TMAH) GC/MS that there is overlap in many of the TMAH products, but also that each stream contained a unique suite of compounds

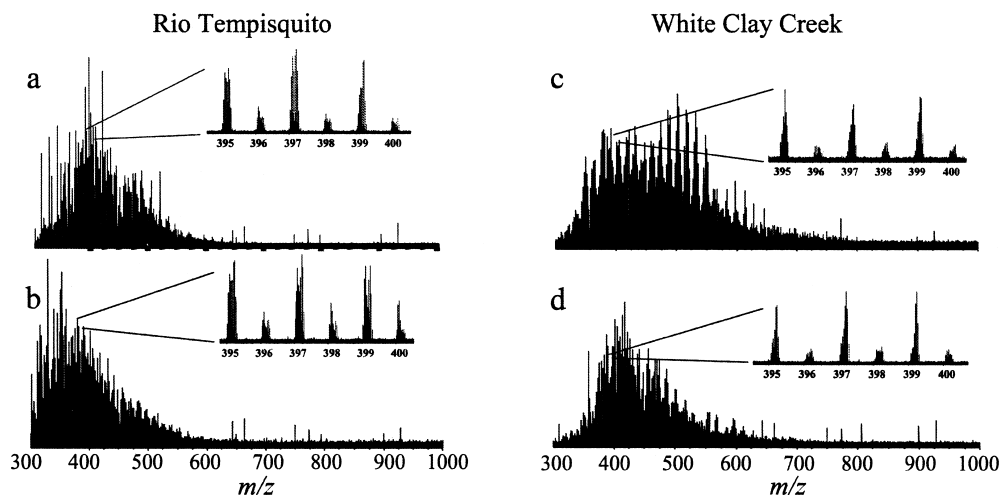


Fig. 1. The ultra-high resolution mass spectra of DOM extracted from (a) inflow and (b) outflow of bioreactors at Rio Tempisquito and (c) inflow and (d) outflow of bioreactors at White Clay Creek.

(Frazier et al. 2005). Given that much of the DOC in these streams is terrestrial in origin and that the two streams arise in biomes with vastly different plant species composition, it follows that DOC within these watersheds should have a distinct molecular character. Additionally, studies of DOC concentrations, flow paths, and land use in pasture, native forests, and tree plantations have shown that the quantity and bioavailability of DOC tends to be higher in near-stream flow paths compared with groundwater sources (Findlay et al. 2001). The proportion of terrestrial DOC delivered to streams from different flow paths also changes during storms (McGlynn and McDonnell 2003). A combination of these factors influences the concentrations and molecular characteristics of DOC and BDOC in our samples. However, with a sample size of two, a precise connection between watershed geochemistry and the molecular structure of DOC is not possible.

**Ultra-high resolution mass spectra**—The calibrated mass spectra of DOM extracted from Rio Tempisquito and White Clay Creek stream waters and their bioreactor effluents reveal over 3,000 peaks (Fig. 1). These peaks represent those whose relative abundances are  $>5\%$  of the base peak and greater than a signal to noise ratio of 5. The distribution of peaks spans the mass range from 300 to 700  $m/z$ . Different instrumental conditions such as lower octopole frequency and longer transfer times between the octopole and ICR cell were attempted to expand the mass range to higher mass. However, no significant improvement in the detection of peaks above 700  $m/z$  was observed. Peaks are observed above 700  $m/z$ , but they are below the 5% threshold and grade into noise. The distribution of peaks from these spectra is consistent with previously published ESI-MS spectra of fulvic acids and DOM from natural water (Plancque et al. 2001; Stenson et al. 2003). Expansions of very narrow mass ranges of the spectra (Fig. 1) highlight the molecular complexity of DOM when one considers that each peak represents at least one or more structures and that there are clusters of peaks at each mass from 300 to 700  $m/z$ . Similar

results are also observed in ESI-FT-ICR mass spectra of humic substances (Kujawinski et al. 2002). The peak resolving power ( $m/\delta m_{50\%}$ ), using peak width at the half maximum peak height ( $\delta m_{50\%}$ ), is calculated to be over 300,000 at around 300  $m/z$ , with an average resolving power of over 200,000 for the entire mass range ( $300 < m/z < 700$ ).

The spectra display a pattern of dominant odd  $m/z$  peaks and weak even  $m/z$  peaks. The majority of peaks at even  $m/z$  can be assigned to the  $^{13}\text{C}$  isotope of peaks at odd  $m/z$  since, in most cases, peaks at even  $m/z$  are identified readily by adding the mass of a neutron to the mass of odd  $m/z$  peaks. Thus, most of the observed peaks at odd  $m/z$  were from singly charged ions, since a similar pattern of corresponding  $^{13}\text{C}$  isotope peaks could be found displaced by exactly the mass of a neutron (Kujawinski et al. 2002). It has been clearly established that singly charged species dominate such spectra (Kujawinski et al. 2002; Stenson et al. 2003), so mass-to-charge ratios simplify to mass.

**Mass distribution**—For both stream waters, visual inspection of the spectra as well as calculations from the spectra show that the distribution of peak heights shifts to a lower mass region after microbial degradation. Visually, we observe two modes in the peak distribution in the spectrum for Rio Tempisquito stream water, a primary mode at a mass of 400 and a secondary mode at a mass of 470 (Fig. 1a). The spectrum obtained from the corresponding outflow water sample displays a mode at 350 Da (Fig. 1b). Similarly, the spectrum acquired from White Clay Creek DOM has a primary mode in its peak distribution at 520 Da and a secondary mode at 370 Da, whereas the peak mode for the outflow showed a decline from the primary mode to one at 420 Da. The values for  $M_w$  and  $M_n$  calculated from the mass spectral distributions of the spectra from stream waters and bioreactor effluents revealed that in Rio Tempisquito,  $M_n$  declined from 430 to 423 Da, whereas  $M_w$  declined from 437 to 429 Da. For White Clay Creek,  $M_n$  declined from 489 to 455 Da and  $M_w$  declined from 502 to 462 Da. The average molecular weight distribution of natural organic matter often has been

expressed as mass-averaged ( $M_w$ ) and/or number-averaged molecular weight values ( $M_n$ ; Chin et al. 1994). Our calculation of  $M_w$  and  $M_n$  assumes that the mass spectra yield representative peak intensities for each individual compound, an assumption that has yet to be tested and is probably not valid based on some recent unpublished work in our group (E. Lee and P.G. Hatcher unpubl. data). Nonetheless, the comparisons can be made assuming that the same general types of molecules are present in inflow and outflow DOM. Additionally, we only consider peaks that are above 5% of base peak intensity. Thus, the  $MW_w$  and  $MW_n$  values are skewed toward lower mass such that comparisons with molecular weight measurements by other techniques are not straightforward. Recent comparisons of ESI-MS data with other molecular weight measurement techniques indicate that the ESI-MS data agree well with NMR-measured molecular weights (Hatcher et al. 2004) but not size exclusion chromatography, vapor pressure osmometry, ultrafiltration, and multiangle light scattering.

There have been conflicting reports in the literature on the relationship between molecular weight of DOM and bioavailability. Investigations with stirred cell ultrafiltration showed a selective utilization of low molecular weight (<10,000 Da) DOM by stream bed sediments followed by a slight increase in the concentration of this smaller size class, presumably representing more refractory moieties remaining from the hydrolysis of larger molecules (Kaplan and Bott 1983). In a large blackwater river, sestonic bacteria used small DOM molecules (<1,000 Da) most effectively, and large molecules more effectively than molecules of intermediate size (Meyer et al. 1987). In another blackwater coastal river, DOM < 1,000 Da supported 4–10 times the respiration compared with DOM >1,000 Da (Covert and Moran 2001). In contrast, studies with marine DOM, examined by tangential flow ultrafiltration, observed the rapid turnover of high molecular weight molecules (>1,000 Da) compared with smaller molecules (Amon and Benner 1994), although monomers must certainly be considered an exception to this phenomenon. In the present study, peaks at high molecular weight (>1,000 Da) are usually either not observed or below the 5% threshold.

The reason for the discrepancy between our findings and those of Amon and Benner (1994)—that >1,000 Da molecular weight material seems to be preferentially utilized—is not entirely clear. First, it is important to consider that these authors used tangential flow ultrafiltration for their studies, and we base our results on the mass spectrometry data for material isolated by  $C_{18}$  extraction. Ultrafiltration is known to preferentially isolate higher molecular weight material, and this material is not observed in the ESI-MS data (Hatcher et al. 2004). There could be limitations or biases in either the  $C_{18}$  extraction procedure or the ESI-MS such that the high molecular weight portion of DOM is not retained, is not ionized efficiently, or is fragmented to lower mass components. Considering the fact that  $C_{18}$ -adsorbent material is routinely used to retain peptides or molecules larger than 1,000 Da, it is unlikely that large molecules would be excluded by this mechanism. One other explanation is that the high-molecular weight material observed by Amon and Benner (1994) is mostly carbohydrate-like material, and we

know that such material has an ionization efficiency in ESI that is quite low compared with more aromatic material from tannins and lignin (E. Lee and P.G. Hatcher unpubl. data). Fragmentation of large aggregates held together by metal bridges or noncovalent interactions in the ESI source is another possible explanation (Hatcher et al. 2004), but the issue remains unresolved and requires further investigation that is beyond the scope of this paper. Nonetheless, for DOM molecules that are <1,000 Da, significant alteration toward lower average molecular weight implies that bioreactor microorganisms are preferentially utilizing the higher molecular weight fraction of this range. We are unable to determine whether the bacteria are converting larger molecules to smaller molecules or mineralizing DOM entirely, although it is likely that both processes are occurring.

*Change of DOM studied by three-dimensional van Krevelen analysis*—The van Krevelen diagrams, constructed from unique elemental formulas from the ultra-high resolution mass spectra indicate consistent trends in the bioreactor inflow and outflow data for the two study streams (Fig. 2). Van Krevelen plots can be used to visualize major biomolecular components of source material such as lipids, lignin, and cellulose (Hedges 1990). In a recent report (Kim et al. 2003a), data from several studies were summarized to diagram the various regions corresponding to major biochemical classes. The data shown in Fig. 2 indicate that there is a primary contribution of peaks in the inflow DOM samples that corresponds to well-known biopolymers such as lignin (H:C = 1.0–1.4, O:C = 0.35–0.50) and tannin (H:C = 0.75–1.4, O:C = 0.35–0.85). Carbohydrates (H:C = 1.5–2.0, O:C = 0.5–1.0); peptides (H:C = 1.6–1.8, O:C = 0.35–0.5); and lipid (H:C = 1.75–2.25, O:C = 0.02–0.15) type material are not represented. Overall, it appears that DOM from White Clay Creek is composed of more oxygenated species since they are located in a higher O:C ratio region. Comparison of DOM molecules in a large number of different stream systems was beyond the scope of this work.

There is overall enhancement of peaks in the lower middle of the plot (H:C = 0.6–0.9, O:C = 0.2–0.4). The effect is greater for bioreactor effluents from Rio Tempisquito. The enhancement of signals in the lower middle part of the plots can be attributed to the relative enrichments in outflow DOM of molecules that have low H:C ratios. This region of the van Krevelen diagram has been assigned to molecules typical of black carbon (BC; Kim et al. 2004), but we also recognized some contributions from tannin-derived species, and our results suggest that the molecules in this presumed black carbon region are refractory to microbial degradation. This finding is consistent with the refractory nature of black carbon (Baldock and Smernik 2002), as well as observations that a decrease in the H:C ratio is a major diagenetic modification influencing DOM in a river system (Sun et al. 1997).

The relative enhancement in the presumed BC-derived peaks appears to be greater for the sample from Rio Tempisquito than it is for White Clay Creek, although the relative degree of biodegradation based on DOC measurements is higher in White Clay Creek. One explanation for this derives from the fact that there is a rich assemblage of molecules in

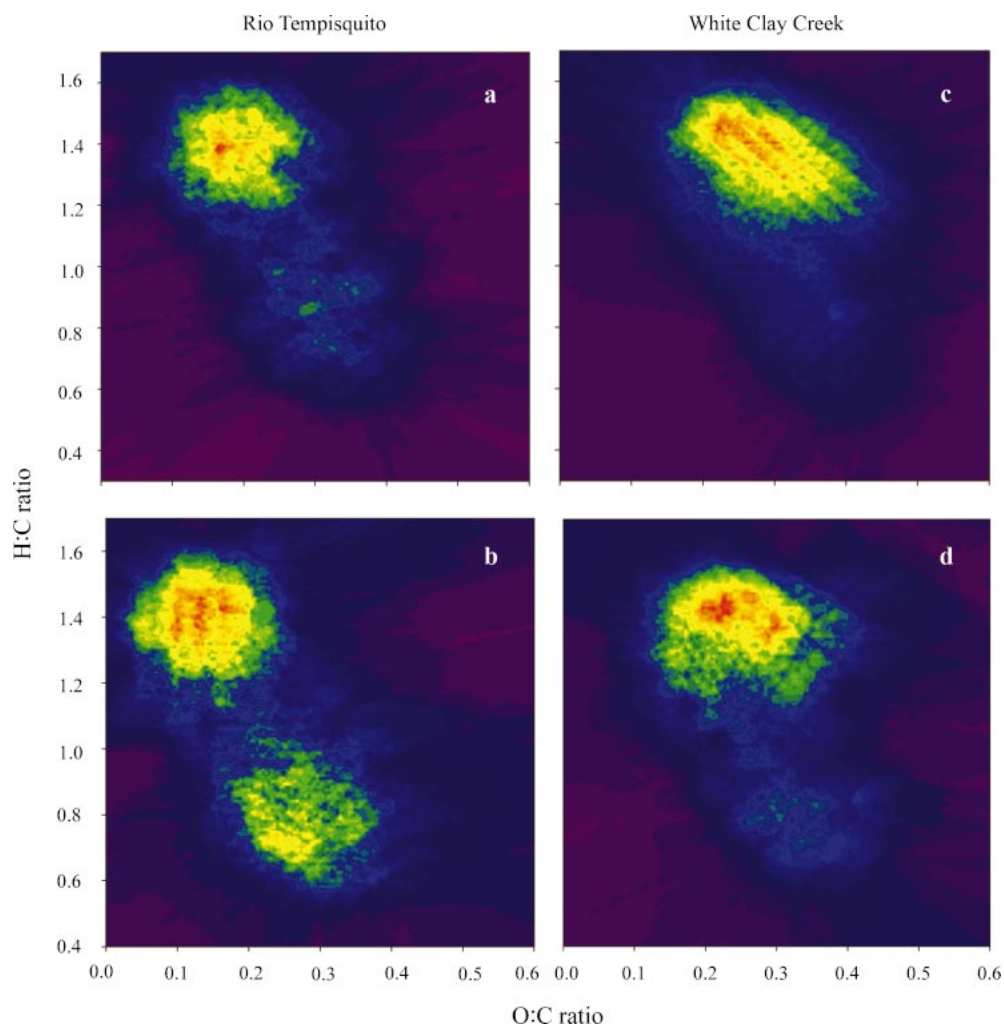


Fig. 2. The van Krevelen diagrams of DOM extracted from (a) inflow and (b) outflow of bioreactors at Rio Tempisquito and (c) inflow and (d) outflow of bioreactors at White Clay Creek.

White Clay Creek DOM that have high H:C ratios and that their biodegradation, while being extensive, leads to undetected small molecules and other molecules that have H:C ratios in the same or slightly different range. In Rio Tempisquito, the amount of available DOM that is palatable to microorganisms may be small and the organisms are well adapted to completely degrade these molecules such that the products are no longer identifiable by mass spectrometry. This leaves the relatively undegraded BC-derived molecules selectively enriched. An alternative explanation is that the ionization efficiencies for non-BC-derived material are much different than for BC-derived material in the two riverine systems. Thus, small changes in DOC at Rio Tempisquito affect the yields of non-BC material much greater than they do at White Clay Creek. Finally, the most likely explanation is that the  $C_{18}$  extraction and ESI mass spectrometry are not representing the biodegradable fraction of DOC as effectively as the BC-derived material. Carbohydrates are an example of a group of molecules that may not be sorbed very readily to  $C_{18}$ . We also know from experiments with model compounds that carbohydrate-like molecules do not

ionize as efficiently as tannin or lignin model compounds (E. Lee and P.G. Hatcher unpubl. data). Thus, the answer to why enhancements in BC-derived molecules do not correlate to BDOC estimates may not be known fully until appropriate experiments are conducted to examine the ionization efficiency of a large range of different molecules under electrospray conditions.

A second trend revealed in the van Krevelen plots was a shift in composition for peaks located toward the top left portion of the plot. The shift primarily involves a change in O:C from a centroid value of 0.2 in inflow DOM from Rio Tempisquito to a centroided value of 0.12 in the respective outflow DOM. This change indicates that biodegradation selectively removes compounds with higher O:C. This effect is also observed in samples from White Clay Creek, but the magnitude of the change is not as much (O:C changes from 0.3 inflow DOM to 0.25 in outflow DOM). Although this observation contrasts with the finding that bacterial growth was inversely related to the O:C ratio, that relationship was driven by data from four fresh plant extracts, with O:C ranging from 0.19 to 0.61, whereas all but one of the stream

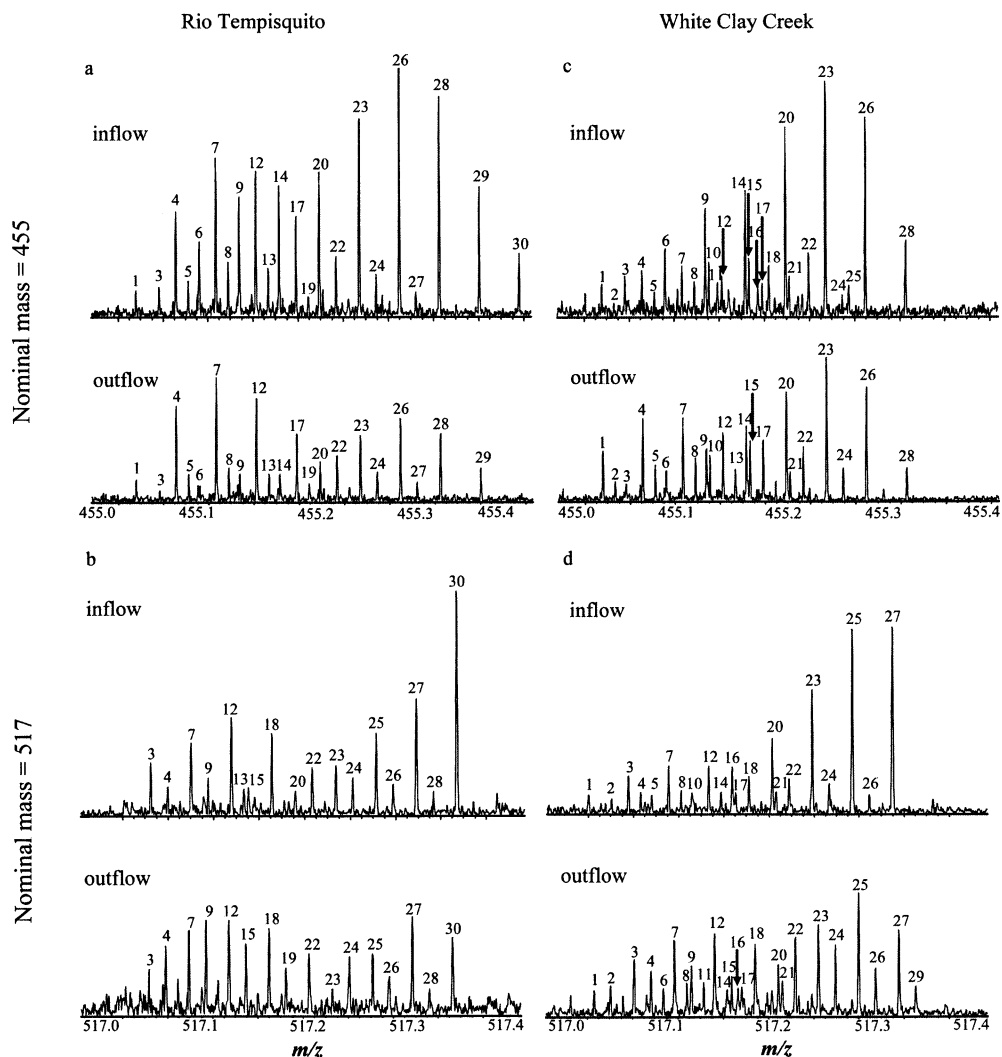


Fig. 3. Expanded region (nominal mass of 455 and 517) of spectra, each obtained from DOM extracted from (a) inflow and (b) outflow of bioreactors at Rio Tempisquito and (c) inflow and (d) outflow of bioreactors at White Clay Creek.

waters had an O:C ratio that was  $>0.63$  (Sun et al. 1997). We suggest that although molecules with low O:C ratios would be more energetically advantageous targets for metabolism, extensively processed molecules exhibiting a high degree of reduction may be less enzymatically accessible. Of course another explanation is that Sun et al. (1997) may have examined DOM that was relatively enriched in carbohydrate-like molecules that have high O:C ratios, and we know that these are not representatively sampled by the ESI-mass spectrometry technique.

*Changes observed in expanded spectra*—The expanded mass spectra for nominal masses of 455 and 517 (Fig. 3) each show about 20 individual peaks for the two streams. The two nominal mass regions of 455 and 517 were rather arbitrarily selected as examples to show changes in expanded mass spectra that are generally repeated for nearly all nominal masses. From the exact masses of these peaks, unique elemental formulas were determined, and these are shown in

Tables 1 and 2. At mass 455, 18 of the peaks were common to both streams, four were unique to Rio Tempisquito, and eight were unique to White Clay Creek. At mass 517, 14 of the peaks were common to both streams, four were unique to Rio Tempisquito, and 12 were unique to White Clay Creek.

The spectra from inflow and outflow water samples of Rio Tempisquito exhibit a striking difference at the selected nominal mass regions in addition to overall changes in spectral features in the entire mass range (Fig. 3a,b). In the inflow sample, the peaks with larger mass defect (deviation from nominal mass) have generally higher peak heights compared with peaks with smaller mass defects. By contrast, the spectrum for the outflow sample shows that the peaks with large mass defects display smaller or, in some cases, only slightly greater intensities. A similar change is observed in spectra from inflow and outflow water samples at White Clay Creek (Fig. 3c,d). In the case of this set of spectra from White Clay Creek, the relative heights of peaks with smaller mass de-

Table 1. Calculated elemental compositions corresponding to peaks from expanded spectra of nominal mass 455, representing samples from Rio Tempisquito (RT) and White Clay Creek (WCC).

Peak no.		Observed mass	Chemical formula	H:C ratio	O:C ratio
RT	WCC				
1	1	455.04079	C <sub>25</sub> H <sub>12</sub> O <sub>9</sub>	0.48	0.36
	2	455.05205	C <sub>24</sub> H <sub>12</sub> N <sub>2</sub> O <sub>8</sub>	0.50	0.33
3	3	455.06186	C <sub>22</sub> H <sub>16</sub> O <sub>11</sub>	0.73	0.50
4	4	455.07715	C <sub>26</sub> H <sub>16</sub> O <sub>8</sub>	0.62	0.31
5	5	455.08839	C <sub>25</sub> H <sub>12</sub> N <sub>6</sub> O <sub>3</sub>	0.64	0.28
6	6	455.0983	C <sub>23</sub> H <sub>20</sub> O <sub>10</sub>	0.87	0.43
7	7	455.11353	C <sub>27</sub> H <sub>20</sub> O <sub>7</sub>	0.74	0.26
8	8	455.12476	C <sub>26</sub> H <sub>20</sub> N <sub>2</sub> O <sub>6</sub>	0.77	0.23
9	9	455.13468	C <sub>24</sub> H <sub>24</sub> O <sub>9</sub>	1.00	0.38
	10	455.13806	C <sub>27</sub> H <sub>22</sub> N <sub>15</sub> O <sub>6</sub>	0.81	0.22
	11	455.14592	C <sub>23</sub> H <sub>24</sub> N <sub>2</sub> O <sub>5</sub>	1.04	0.35
12	12	455.14992	C <sub>28</sub> H <sub>24</sub> O <sub>6</sub>	0.86	0.21
13	13	455.16117	C <sub>27</sub> H <sub>24</sub> N <sub>2</sub> O <sub>5</sub>	0.89	0.19
14	14	455.17109	C <sub>25</sub> H <sub>28</sub> O <sub>8</sub>	1.12	0.32
	15	455.17447	C <sub>29</sub> H <sub>22</sub> N <sub>5</sub> O <sub>1</sub>	0.76	0.03
	16	455.1825	C <sub>24</sub> H <sub>28</sub> N <sub>2</sub> O <sub>7</sub>	1.17	0.29
17	17	455.18638	C <sub>29</sub> H <sub>28</sub> O <sub>5</sub>	0.97	0.17
	18	455.19232	C <sub>22</sub> H <sub>32</sub> O <sub>10</sub>	1.45	0.45
19		455.19735	C <sub>28</sub> H <sub>28</sub> N <sub>2</sub> O <sub>4</sub>	1.00	0.14
20	20	455.20751	C <sub>26</sub> H <sub>32</sub> O <sub>7</sub>	1.23	0.27
	21	455.21089	C <sub>15</sub> H <sub>32</sub> N <sub>6</sub> O <sub>10</sub>	2.13	0.67
22	22	455.22282	C <sub>30</sub> H <sub>32</sub> O <sub>4</sub>	1.07	0.13
23	23	455.2439	C <sub>27</sub> H <sub>36</sub> O <sub>6</sub>	1.33	0.22
24	24	455.25914	C <sub>31</sub> H <sub>36</sub> O <sub>3</sub>	1.16	0.10
	25	455.26508	C <sub>24</sub> H <sub>40</sub> O <sub>8</sub>	1.67	0.33
26	26	455.28027	C <sub>28</sub> H <sub>40</sub> O <sub>5</sub>	1.43	0.18
	27	455.29575	C <sub>32</sub> H <sub>40</sub> O <sub>2</sub>	1.25	0.06
28	28	455.3167	C <sub>29</sub> H <sub>44</sub> O <sub>4</sub>	1.52	0.14
29		455.35325	C <sub>30</sub> H <sub>48</sub> O <sub>3</sub>	1.60	0.10
30		455.3896	C <sub>31</sub> H <sub>52</sub> O <sub>2</sub>	1.68	0.06

Table 2. Calculated elemental compositions corresponding to peaks from expanded spectra of nominal mass 517, representing samples from Rio Tempisquito (RT) and White Clay Creek (WCC).

Peak no.		Observed mass	Chemical formula	H:C ratio	O:C ratio
RT	WCC				
	1	517.04132	C <sub>26</sub> H <sub>14</sub> O <sub>12</sub>	0.54	0.46
	2	517.056118	C <sub>30</sub> H <sub>14</sub> O <sub>9</sub>	0.47	0.30
3	3	517.07750	C <sub>27</sub> H <sub>18</sub> O <sub>11</sub>	0.67	0.41
4	4	517.09285	C <sub>31</sub> H <sub>18</sub> O <sub>8</sub>	0.58	0.26
	5	517.09864	C <sub>24</sub> H <sub>22</sub> O <sub>13</sub>	0.92	0.54
	6	517.10413	C <sub>30</sub> H <sub>18</sub> N <sub>2</sub> O <sub>7</sub>	0.60	0.23
7	7	517.11396	C <sub>28</sub> H <sub>22</sub> O <sub>10</sub>	0.79	0.36
	8	517.12522	C <sub>27</sub> H <sub>22</sub> N <sub>2</sub> O <sub>9</sub>	0.81	0.33
9	9	517.12934	C <sub>32</sub> H <sub>22</sub> O <sub>7</sub>	0.69	0.22
	10	517.13509	C <sub>25</sub> H <sub>26</sub> O <sub>12</sub>	1.04	0.48
	11	517.14048	C <sub>31</sub> H <sub>22</sub> N <sub>2</sub> O <sub>6</sub>	0.71	0.19
12	12	517.15034	C <sub>29</sub> H <sub>26</sub> O <sub>9</sub>	0.90	0.31
13	13	517.16103	C <sub>27</sub> H <sub>20</sub> N <sub>9</sub> O <sub>3</sub>	0.74	0.11
	14	517.16164	C <sub>28</sub> H <sub>25</sub> N <sub>2</sub> O <sub>8</sub>	0.89	0.29
15	15	517.16577	C <sub>33</sub> H <sub>26</sub> O <sub>6</sub>	0.79	0.18
	16	517.17159	C <sub>26</sub> H <sub>30</sub> O <sub>11</sub>	1.15	0.42
	17	517.17494	C <sub>30</sub> H <sub>24</sub> N <sub>5</sub> O <sub>4</sub>	0.80	0.13
18	18	517.18683	C <sub>30</sub> H <sub>30</sub> O <sub>8</sub>	1.00	0.27
19		517.20161	C <sub>34</sub> H <sub>30</sub> O <sub>5</sub>	0.85	0.15
20	20	517.20796	C <sub>27</sub> H <sub>34</sub> O <sub>10</sub>	1.26	0.37
	21	517.21157	C <sub>31</sub> H <sub>27</sub> N <sub>5</sub> O <sub>3</sub>	0.87	0.10
22	22	517.22322	C <sub>31</sub> H <sub>34</sub> O <sub>7</sub>	1.10	0.23
23	23	517.24435	C <sub>28</sub> H <sub>38</sub> O <sub>9</sub>	1.36	0.32
24	24	517.25953	C <sub>32</sub> H <sub>38</sub> O <sub>6</sub>	1.19	0.19
25	25	517.28078	C <sub>29</sub> H <sub>42</sub> O <sub>8</sub>	1.45	0.28
26	26	517.29604	C <sub>33</sub> H <sub>42</sub> O <sub>5</sub>	1.27	0.15
27	27	517.31716	C <sub>30</sub> H <sub>46</sub> O <sub>7</sub>	1.53	0.23
28		517.33150	C <sub>32</sub> H <sub>44</sub> N <sub>2</sub> O <sub>3</sub>	1.38	0.09
	29	517.33238	C <sub>34</sub> H <sub>46</sub> O <sub>4</sub>	1.35	0.12
30		517.35291	C <sub>31</sub> H <sub>50</sub> O <sub>6</sub>	1.61	0.19

fects are relatively increased in outflow DOM compared with inflow DOM. Considering the fact that hydrogen and oxygen will have the greatest influence on overall mass defect (deviation from nominal mass), the molecules that correspond to the peaks near nominal masses can be expected to have a relatively small number of hydrogen atoms combined with larger numbers of oxygen atoms. Accordingly, the peaks with low mass defects tend to have low molar H:C ratios and/or high O:C ratios (Tables 1 and 2), and they can be related to suggested structures of degraded black carbon molecules (Kim et al. 2004).

There are some peaks that do not follow this pattern. For example, although peaks 9 and 14 in Fig. 3a,b have relatively small mass defects, the relative intensity of these peaks is decreased from inflow to outflow DOM samples. From Table 1, it is clear that those peaks have H:C ratio values  $\geq 1.0$ . On the other hand, peaks 1, 3, 4, and 6 with lower H:C ratios ( $< 0.8$ ) are relatively increased in height compared with peaks with higher H:C ratios from inflow to outflow DOM samples. The peaks with larger mass defects generally have H:C ratios  $> 1$  (for example, peaks 23, 26, 28, 29, and 30 in Fig. 3a,b) and show a decrease in intensity. It is clear that the relative importance of some peaks, corresponding to H-deficient molecules (molecules with low H:

C ratios), is increased from inflow to outflow water samples compared with that of peaks with higher H:C ratios. The same trend has been observed for the expanded mass spectra of nominal mass of 517. Peaks with H:C ratio values  $> 1$  (for example, peaks 20, 23, 25, 27, and 30 in Fig. 3c,d) show a decrease from inflow to outflow samples. The trend observed in the two mass regions generally holds for the entire mass range and correlates well with what is observed in the van Krevelen analysis for the entire spectrum.

In a previous study (Kim et al. 2004), we suggested that the BC-derived molecules might survive degradation and be exported to the oceans. This conclusion assumes that they would not be biodegraded or photodegraded. Lacking evidence for biodegradation, we set out to examine the bioresistivity of these BC-derived molecules. In this study, we demonstrate that the type of molecules assigned to BC in our previous study are more resistant to biodegradation than non-BC molecules. This same trend for DOM is observed in the two different stream systems investigated. The molecular-level evidence suggesting survival from biodegradation of BC molecules in riverine systems is a key requirement for speculating that these types of molecules will eventually flow into the ocean. Mannino and Harvey (2004) had suggested that BC is being exported from large water-

sheds along the eastern United States, and an important requirement for the export to be significant is the recalcitrance of BC within the watershed, which our data appear to show.

Several important questions remain related to our current findings. We are unable to (1) assess whether the refractory carbon is young ( $^{14}\text{C}$ -rich) or old ( $^{14}\text{C}$ -depleted); (2) assign structures to compounds whose elemental formulas we have revealed; and (3) quantitate the changes in the concentrations of individual molecules. Isotopic analyses of DOC and particulate OC in samples from eight large rivers showed that the younger portion of terrestrial organic matter is selectively degraded compared with the older DOM (Raymond and Bauer 2001). Investigations in the York River estuary and Hudson River, including analyses of bacterial nucleic acids, revealed that both young and relic organic matter supports heterotrophy in large rivers (McCallister et al. 2004). Similarly, an analysis of  $\text{CO}_2$  outgassing from rivers within the Amazon basin revealed that the vast majority of organic matter respired is young, yet much of the older organic matter also is metabolized in transit to the ocean (Mayorga et al. 2005).

Prior characterizations of BDOC with TMAH GC/MS and bioreactors, although novel and informative, do not provide the full molecular-level description of this method, especially for hydrophobic constituents. The TMAH GC/MS approach relies on base hydrolysis and simultaneous methylation to provide structural information for monomer constituents of DOM, whereas the ESI-FT-ICR-MS method described here is nondestructive but lacks specific structural detail beyond elemental composition. Thus, attempts to compare and contrast information from these two different approaches are not likely to be successful. We can postulate that the hydrogen-deficient molecules identified in this study are not observed with TMAH GC/MS, or other molecular-level GC/MS-based characterization techniques commonly used for DOM, because such molecules would not be volatile enough for GC/MS analysis, even if they were fully methylated. Studies that combine chemical and isotopic analyses with improvements to make this ESI-FT-ICR-MS method quantitative will help improve our understanding of the global carbon cycle and facilitate the development of ecosystem-level models of energy flow.

## References

- AMON, R. M. W., AND R. BENNER. 1994. Rapid-cycling of high-molecular-weight dissolved organic matter in the ocean. *Nature* **369**: 549–552.
- BALDOCK, J. A., AND R. J. SMERNIK. 2002. Chemical composition and bioavailability of thermally altered *Pinus resinosa* (red pine) wood. *Org. Geochem.* **33**: 1093–1109.
- BRINSON, M. M. 1976. Organic matter losses from four watersheds in the humid tropics. *Limnol. Oceanogr.* **21**: 572–582.
- BROWN, T. L., AND J. A. RICE. 2000. Effect of experimental parameters on the ESI-FT-ICR mass spectrum of fulvic acid. *Anal. Chem.* **72**: 384–390.
- CHIN, Y. P., G. AIKEN, AND E. OLOUGHLIN. 1994. Molecular-weight, polydispersity, and spectroscopic properties of aquatic humic substances. *Environ. Sci. Technol.* **28**: 1853–1858.
- COVERT, J. S., AND M. A. MORAN. 2001. Molecular characterization of estuarine bacterial communities that use high- and low-molecular weight fractions of dissolved organic carbon. *Aquat. Microb. Ecol.* **25**: 127–139.
- FINDLAY, S., J. M. QUINN, C. W. HICKEY, G. BURRELL, AND M. DOWNES. 2001. Effects of land use and riparian flowpath on delivery of dissolved organic carbon to streams. *Limnol. Oceanogr.* **46**: 345–355.
- FRAZIER, S. W., L. A. KAPLAN, AND P. G. HATCHER. 2005. The molecular characterization of biodegradable dissolved organic matter using bioreactors and [ $^{12}\text{C}/^{13}\text{C}$ ] tetramethylammonium hydroxide thermochemolysis GC-MS. *Environ. Sci. Technol.* **39**: 1479–1491.
- HATCHER, P. G., S. KIM, AND Y. SUGIYAMA. 2004. Intercomparisons of some new approaches for investigating the molecular weight distribution of dissolved organic matter, p. 241–243. *In* L. Martin-Neto, D. M. B. P. Milori, and W. T. L. de Silva [eds.], *Humic substances and soil and water environment*. Embrapa.
- HEDGES, J. I. 1990. Compositional indicators of organic acid sources and reactions in natural environments, p. 43–63. *In* E. M. Perdue and E. T. Gjessing [eds.], *Organic acids in aquatic ecosystems*. Wiley.
- KAPLAN, L. A., AND T. L. BOTT. 1983. Microbial heterotrophic utilization of dissolved organic matter in a piedmont stream. *Freshwater Biol.* **13**: 363–377.
- , AND J. D. NEWBOLD. 1995. Measurement of streamwater biodegradable dissolved organic carbon with a plug-flow bioreactor. *Water Res.* **29**: 2696–2706.
- KIM, S., L. A. KAPLAN, R. BENNER, AND P. G. HATCHER. 2004. Hydrogen-deficient molecules in natural riverine water samples—evidence for the existence of black carbon in DOM. *Mar. Chem.* **92**: 225–234.
- , R. W. KRAMER, AND P. G. HATCHER. 2003a. Graphical method for analysis of ultrahigh-resolution broadband mass spectra of natural organic matter, the Van Krevelen diagram. *Anal. Chem.* **75**: 5336–5344.
- , A. SIMPSON, E. B. KUJAWINSKI, M. A. FREITAS, AND P. G. HATCHER. 2003b. Non-invasive advanced spectroscopic methods (electrospray ionization mass spectrometry and 2D solution NMR) for analysis of DOM isolated by  $\text{C}_{18}$  solid phase disk extraction. *Org. Geochem.* **34**: 1325–1335.
- KOCH, B. P., M. WITT, R. ENGBRODT, T. DITTMAR, AND G. KATTNER. 2005. Molecular formulae of marine and terrigenous dissolved organic matter detected by electrospray ionization Fourier transform ion cyclotron resonance mass spectrometry. *Geochim. Cosmochim. Acta* **69**: 3299–3308.
- KUJAWINSKI, E. B., P. G. HATCHER, AND M. A. FREITAS. 2002. High-resolution Fourier transform ion cyclotron resonance mass spectrometry (FT-ICR-MS) of humic and fulvic acids: Improvements and comparisons. *Anal. Chem.* **74**: 413–419.
- MANNINO, A., AND H. R. HARVEY. 2004. Black carbon in estuarine and coastal ocean dissolved organic matter. *Limnol. Oceanogr.* **49**: 735–740.
- MAYORGA, E., AND OTHERS. 2005. Young organic matter as a source of carbon dioxide outgassing from Amazonian rivers. *Nature* **436**: 538–541.
- MCCALLISTER, S. L., J. E. BAUER, J. E. CHERRIER, AND H. W. DUCKLOW. 2004. Assessing sources and ages of organic matter supporting river and estuarine bacterial production: A multiple-isotope ( $\delta^{14}\text{C}$ ,  $\delta^{13}\text{C}$ , and  $\delta^{15}\text{N}$ ) approach. *Limnol. Oceanogr.* **49**: 1687–1702.
- MCGLYNN, B. L., AND J. J. McDONNELL. 2003. Role of discrete landscape units in controlling catchment dissolved organic carbon dynamics. *Water Resour. Res.* **39**, 1090[doi:10.29129/2002WR001525].
- MEYER, J. L., R. T. EDWARDS, AND R. RISLEY. 1987. Bacterial growth on dissolved organic carbon from a blackwater river. *Microb. Ecol.* **13**: 13–29.

- MORERA, A. V. 1983. Soils, p. 63–65. *In* D. H. Janzen [ed.], Costa Rican natural history. Univ. of Chicago Press.
- PLANCQUE, G., B. AMEKRAZ, V. MOULIN, P. TOULHOAT, AND C. MOULIN. 2001. Molecular structure of fulvic acids by electrospray with quadrupole time-of-flight mass spectrometry. *Rapid Commun. Mass Spectrom.* **15**: 827–835.
- RAYMOND, P. A., AND J. E. BAUER. 2001. Riverine export of aged terrestrial organic matter to the north Atlantic ocean. *Nature* **409**: 497–500.
- SEITZINGER, S. P., H. HARTNETT, R. LAUCK, M. MAZUREK, T. MINOGISHI, G. SPYRES, AND R. STYLES. 2005. Molecular level chemical characterization and bioavailability of dissolved organic matter in streamwater using ESI mass spectrometry. *Limnol. Oceanogr.* **50**: 1–12.
- STENSON, A. C., A. G. MARSHALL, AND W. T. COOPER. 2003. Exact masses and chemical formulas of individual Suwannee River fulvic acids from ultrahigh resolution electrospray ionization Fourier transform ion cyclotron resonance mass spectra. *Anal. Chem.* **75**: 1275–1284.
- SUN, L., E. M. PERDUE, J. L. MEYER, AND J. WEIS. 1997. Use of elemental composition to predict bioavailability of dissolved organic matter in a Georgia river. *Limnol. Oceanogr.* **42**: 714–721.
- VAN KREVELEN, D. W. 1950. Graphical-statistical method for the study of structure and reaction processes of coal. *Fuel* **29**: 269–284.
- VOLK, C. J., C. B. VOLK, AND L. A. KAPLAN. 1997. Chemical composition of biodegradable dissolved organic matter in streamwater. *Limnol. Oceanogr.* **42**: 39–44.
- WHITTAKER, R. H., AND G. E. LIKENS. 1973. Carbon in the biota, p. 281–302. *In* G. M. Woodwell and E. V. Pecan [eds.], Carbon and the biosphere. U.S. Atomic Energy Commission.

*Received: 7 January 2005*

*Accepted: 29 August 2005*

*Amended: 21 October 2005*